# Theory of Multipath Shape Factors for Small-Scale Fading Wireless Channels

Gregory D. Durgin, *Student Member, IEEE,* and Theodore S. Rappaport, *Fellow, IEEE*

***Abstract*—This paper presents a new theory of multipath shape factors that greatly simplifies the description of small-scale fading statistics of a wireless receiver. A method is presented for reducing a multipath channel with arbitrary spatial complexity to three shape factors that have simple intuitive geometrical interpretations. Furthermore, these shape factors are shown to describe the statistics of received signal fluctuations in a fading multipath channel. Analytical expressions for level-crossing rate, average fade duration, envelope autocovariance, and coherence distance are all derived using the new shape factor theory and then applied to several classical examples for comparison.**

***Index Terms*—Angle of arrival, diversity, fading channels, mobile communications, multipath channels, propagation, scattering.**

## I. Introduction

THE motion in space of a wireless receiver operating in a multipath channel results in a communications link that experiences small-scale fading. The term *small-scale fading* describes the rapid fluctuations of received power level due to small subwavelength changes in receiver position [1]. This effect is due to the constructive and destructive interference of the numerous multipath waves that impinge upon a wireless receiver [2]. The resulting signal strength fluctuations affect, in some way, nearly every aspect of receiver design: dynamic range, equalization, diversity, modulation scheme, and channel and error-correction coding.

Due to its random unpredictable nature, small-scale fading is always studied as a stochastic process. Numerous researchers have measured and analyzed the *first-order* statistics of these processes, which mostly involves the characterization of small-scale fading with a probability density function (PDF) [3]–[5]. The autocorrelation statistics of fading processes or *second-order* statistics have also been studied [6], [7]. Second-order statistics include measures of a process such as power spectral density (PSD), level-crossing rate, and average fade duration.

Second-order statistics are heavily dependent on the angles-of-arrival of received multipath. Traditionally, most second-order statistics have been studied using an omnidirectional azimuthal propagation model [2]. That is, multipath waves are assumed to arrive at the receiver with equal power from the horizon in every possible direction. Truthfully, no realistic channel resembles this idealized model, but it does approximate multipath propagation for receivers operating in heavily shadowed regions with a dense concentration of scatterers and yields analytical results which resembled early field measurements [6]. The model has the added bonus of producing analytical statistics that are isotropic, unrealistically identical regardless of the direction traveled by the mobile receiver. Unfortunately, recent measurements and models have shown that the arriving multipath of a local area bears little resemblance to the omnidirectional propagation assumption [8], [9]. Moreover, even an approximately omnidirectional channel will no longer appear as such if directional or smart antenna systems are employed at the receiver [10], [11].

This paper augments the classical theory of small-scale fading by introducing the new concept of *multipath shape factors,* which allow the quantitative analysis of *any* distribution of nonomnidirectional multipath waves in a local area (where the signal strength is assumed to be wide-sense stationary). Three principle shape factors—the angular spread, the angular constriction, and the azimuthal direction of maximum fading—are defined and exactly related to the average rate at which a received signal fades [12]. Four of the basic second-order small-scale fading statistics—level-crossing rate, average fade duration, autocovariance, and coherence distance—are then derived using the multipath shape factor theory. To demonstrate the accuracy and simplicity of the theory, several classical propagation problems are analyzed using multipath shape factors. This paper provides a principle contribution by presenting a fundamental, intuitive and quantitative description of how nonomnidirectional multipath affects the second-order statistics of small-scale fading.

## II. Multipath Shape Factors

This section presents the three multipath shape factors that influence second-order fading statistics. The shape factors are derived from the angular distribution of multipath power, $p(\theta)$, which is a general representation of from-the-horizon propagation in a local area [7]. This representation of $p(\theta)$ includes antenna gains and polarization mismatch effects [13]. Shape factors are based on the complex Fourier coefficients of $p(\theta)$

$$F_n = \int_0^{2\pi} p(\theta_x)\, \exp(jn\theta_x)\, d\theta_x \tag{1}$$

where $F_n$ is the $n$th complex Fourier coefficient. The utility of these three shape factors is made apparent in Section III.

Manuscript received May 3, 1999; revised November 3, 1999. This work was supported by a Bradley Fellowship in Electrical Engineering and the MPRG Industrial Affiliates Program. This work was presented in part at the 1999 IEEE Vehicular Technology Conference, Houston, TX, May 1999; at PIMRC 99, Osaka, Japan, September 1999; and at Globecom 99, Rio de Janeiro, Brazil, December 1999.

The authors are with the Mobile and Portable Radio Research Group, Bradley Department of Electrical and Computer Engineering, Virginia Polytechnic Institute and State University, Blacksburg, VA 24061-0350 USA.

Publisher Item Identifier S 0018-926X(00)03257-9.

### A. Angular Spread $\Lambda$

The shape factor *angular spread* $\Lambda$ is a measure of how multipath concentrates about a single azimuthal direction. We define angular spread to be

$$\Lambda = \sqrt{1 - \frac{|F_1|^2}{F_0^2}} \tag{2}$$

where $F_0$ and $F_1$ are defined by (1). There are several advantages to defining angular spread in this manner. First, since angular spread is normalized by $F_0$ (the total amount of local average received power), it is invariant under changes in transmitted power. Second, $\Lambda$ is invariant under any series of rotational or reflective transformations of $p(\theta)$. Finally, this definition is intuitive; angular spread ranges from zero to one, with zero denoting the extreme case of a single multipath component from a single direction and one denoting no clear bias in the angular distribution of received power.

It should be noted that other definitions exist in the literature for angular spread. These definitions involve either beamwidth or the RMS $\theta$ calculations and are often ill suited for general application to periodic functions such as $p(\theta)$ [14]–[17].

### B. Angular Constriction $\gamma$

The shape factor *angular constriction* $\gamma$ is a measure of how multipath concentrates about *two* azimuthal directions. We define angular constriction to be

$$\gamma = \frac{\left|F_0 F_2 - F_1^2\right|}{F_0^2 - |F_1|^2} \tag{3}$$

where $F_0$, $F_1$, and $F_2$ are defined by (1). Much like the definition of angular spread, the measure for angular constriction is invariant under changes in transmitted power or any series of rotational or reflective transformations of $p(\theta)$. The possible values of angular constriction $\gamma$ range from zero to one, with zero denoting no clear bias in two arrival directions and one denoting the extreme case of exactly two multipath components arriving from different directions.

### C. Azimuthal Direction of Maximum Fading $\theta_{\max}$

A third shape factor, which may be thought of as an orientation parameter, is the *azimuthal direction of maximum fading* $\theta_{\max}$. We define this parameter to be

$$\theta_{\max} = \tfrac{1}{2} \arg\left\{F_0 F_2 - F_1^2\right\}. \tag{4}$$

The physical meaning of the parameter is presented in the next section.

## III. Rate Variance Relationships

Complex received voltage, received power, and received envelope are the three basic stochastic processes that are studied in a small-scale fading analysis. In order to understand how these stochastic processes evolve over space, it is useful to study the position derivatives or rate-of-changes of the three processes. Since the mean derivative of a stationary process is zero, the mean-squared derivative is the simplest statistic that measures the fading rate of a channel. In fact, a mean-squared derivative of a stationary process is actually the *variance* of the rate-of-change. This section, therefore, presents equations for describing the rate variance relationships of small-scale received complex voltage, power, and envelope fluctuations. All of these relationships are proven exactly in Appendix I.

### A. Complex Received Voltage $\tilde{V}(r)$

The complex received voltage $\tilde{V}(r)$ is a base-band representation of the summation of numerous multipath waves that have impinged upon the receiver antenna and have excited a complex voltage component at the input of a receiver [1]. Appendix I-A derives the rate variance $\sigma^2_{\tilde{V}'}$ for the complex voltage of a receiver traveling along the azimuthal direction $\theta$

$$\begin{aligned}\sigma^2_{\tilde{V}'}(\theta) &= E\left\{\left|\frac{d\tilde{V}(r)\exp(-jk_c r)}{dr}\right|^2\right\} \\ &= \frac{2\pi^2\Lambda^2 P_T}{\lambda^2}\left(1+\gamma\cos[2(\theta-\theta_{\max})]\right)\end{aligned} \tag{5}$$

where $\lambda$ is the wavelength of the carrier frequency, $P_T$ is the mean-squared received power (units of *volts squared*), and $k_c$ is the centroid of the complex voltage power spectrum (removes any nonzero linear phase taper). Note that the dependence on multipath angle-of-arrival in (5) may be reduced entirely to the three basic shape factors: angular spread, angular constriction, and the azimuthal direction of maximum fading. The physical significance of $\sigma^2_{\tilde{V}'}$ is that it describes the spatial selectivity of a channel in a local area and, by extension, the average complex voltage fluctuations for a mobile receiver.

### B. Received Power $P(r)$

Received power $P(r)$ is equal to the magnitude-squared of complex voltage $\tilde{V}(r)$. Note that this definition of power yields units of *volts squared* rather than *watts*, which would differ only by a constant of proportionality related to the input impedance of the receiver; the *volts-squared* definition is more general and independent of the receiver used.

The mathematical operation of taking the squared magnitude of a complex quantity is a nonlinear operation, so in order to derive a rate variance relationship for received power, we will assume that the channel is *Rayleigh fading*. This assumption, however, is unnecessary for the derivation of (5). Appendix I-B derives the rate variance $\sigma^2_{P'}$ for the power of a receiver traveling along the azimuthal direction $\theta$

$$\begin{aligned}\sigma^2_{P'}(\theta) &= E\left\{\left(\frac{dP(r)}{dr}\right)^2\right\} \\ &= \frac{4\pi^2\Lambda^2 P_T^2}{\lambda^2}\left(1+\gamma\cos[2(\theta-\theta_{\max})]\right).\end{aligned} \tag{6}$$

Once again, the dependence on multipath angle-of-arrival in (6) may be reduced entirely to the three basic shape factors. The physical significance of $\sigma^2_{P'}$ is that it describes the average received power fluctuations in a Rayleigh fading local area.

### C. Received Envelope $R(r)$

Received envelope $R(r)$ is equal to the magnitude of complex voltage $\tilde{V}(r)$. Once again, we will assume that the channel

is *Rayleigh fading* to calculate the mean-squared fading rate. Appendix I-C shows how this assumption leads to the envelope rate variance $\sigma^2_{R'}$

$$\sigma^2_{R'}(\theta) = E\left\{\left(\frac{dR(r)}{dr}\right)^2\right\} = \frac{\pi^2\Lambda^2 P_T}{\lambda^2}\left(1+\gamma\cos[2(\theta-\theta_{\max})]\right). \quad (7)$$

Again, (7) depends on $\Lambda$, $\gamma$, and $\theta_{\max}$. The physical significance of $\sigma^2_{R'}$ is that it describes the average envelope fluctuations in a Rayleigh fading local area.

### D. Comparison to Omnidirectional Propagation

Applying the three shape factors $\Lambda$, $\gamma$, and $\theta_{\max}$ to the classical omnidirectional propagation model, we find that there is not a bias in either one or two directions of angle-of-arrival, leading to maximum angular spread ($\Lambda = 1$) and minimum angular constriction ($\gamma = 0$). The statistics of omnidirectional propagation are *isotropic*, exhibiting no dependence on the azimuthal direction of receiver travel $\theta$.

If the rate variance relationships of (5)–(7) are normalized against their values for omnidirectional propagation, then they reduce to the following form:

$$\overline{\sigma}^2(\theta) = \frac{\sigma^2_{\dot{V}'}(\theta)}{\sigma^2_{\dot{V}'(\text{omni})}} = \frac{\sigma^2_{P'}(\theta)}{\sigma^2_{P'(\text{omni})}} = \frac{\sigma^2_{R'}(\theta)}{\sigma^2_{R'(\text{omni})}} = \Lambda^2(1+\gamma\cos[2(\theta-\theta_{\max})]) \quad (8)$$

where $\overline{\sigma}^2$ is a normalized fading rate variance. Equation (8) provides a convenient way to analyze the effects of the shape factors on the second-order statistics of small-scale fading.

First, notice that angular spread $\Lambda$ describes the *average* fading rate within a local area. A convenient way of viewing this effect is to consider the fading rate variance taken along two perpendicular directions within the same local area. From (8), the average of the two fading rate variances, regardless of the orientation of the measurement, is always given by

$$\tfrac{1}{2}\left[\overline{\sigma}^2(\theta)+\overline{\sigma}^2(\theta+\pi/2)\right] = \Lambda^2. \quad (9)$$

Equation (9) clearly shows that the average fading rate within a local area decreases with respect to omnidirectional propagation as multipath power becomes more and more concentrated about a single azimuthal direction. A method for measuring multipath angular spread based on this relationship has been presented in [18].

Second, notice that angular constriction $\gamma$ does not affect the average fading rate within a local area, but describes the variability of fading rates taken along different azimuthal directions $\theta$. From (8), fading rate variance $\overline{\sigma}^2$ will change as a function of direction of receiver travel $\theta$, but will always fall within the following range:

$$\sqrt{1-\gamma} \le \frac{\overline{\sigma}(\theta)}{\Lambda} \le \sqrt{1+\gamma}. \quad (10)$$

The upper limit of (10) corresponds to a receiver traveling in the azimuthal direction of maximum fading ($\theta = \theta_{\max}$) while the lower limit corresponds to travel in a perpendicular direction ($\theta = \theta_{\max} + \pi/2$). Equation (10) clearly shows that the variability of fading rates within the same local area increases as the channel becomes more and more constricted.

It is interesting to note that the propagation mechanisms of a channel are not uniquely described by the three shape factors $\Lambda$, $\gamma$, and $\theta_{\max}$. An infinitum of propagation mechanisms exist which may have the same set of shape factors and, by extension, lead to channels which exhibit nearly the same end-to-end performance. In fact, (8) provides rigorous mathematical criteria for a multipath channel that may be treated as "pseudo-omnidirectional"

$$|F_1|,\ |F_2| \ll F_0. \quad (11)$$

Under the condition of (11), angular spread becomes approximately one and angular constriction becomes approximately zero. Thus, the second-order statistics of the channel behave nearly identical to the classical omnidirectional channel.

## IV. Examples of Fading Behavior

This section presents four different analytical examples of nonomnidirectional propagation channels that provide insight into the shape factor definitions and how they describe fading rates.

### A. Two-Wave Channel Model

Consider the simplest small-scale fading situation where two coherent, constant-amplitude multipath components, with individual powers defined by $P_1$ and $P_2$, arrive at a mobile receiver separated by an azimuthal angle $\alpha$. Fig. 1 illustrates this angular distribution of power, which is mathematically defined as

$$p(\theta) = P_1\delta(\theta-\theta_o) + P_2\delta(\theta-\theta_o-\alpha) \quad (12)$$

where $\theta_o$ is an arbitrary offset angle and $\delta(\cdot)$ is an impulse function. By applying (2)–(4), the expressions for $\Lambda$, $\gamma$, and $\theta_{\max}$ for this distribution are

$$\Lambda = \frac{2\sqrt{P_1P_2}}{P_1+P_2}\sin\frac{\alpha}{2}, \qquad \gamma = 1, \qquad \theta_{\max} = \theta_0 + \frac{\alpha+\pi}{2}. \quad (13)$$

The angular constriction $\gamma$ is always one because the two-wave model represents perfect clustering about two directions. The limiting case of two multipath components arriving from the same direction ($\alpha = 0$) results in an angular spread $\Lambda$ of zero. An angular spread of one results only when two multipath of identical powers ($P_1 = P_2$) are separated by $\alpha = 180°$. Fig. 1

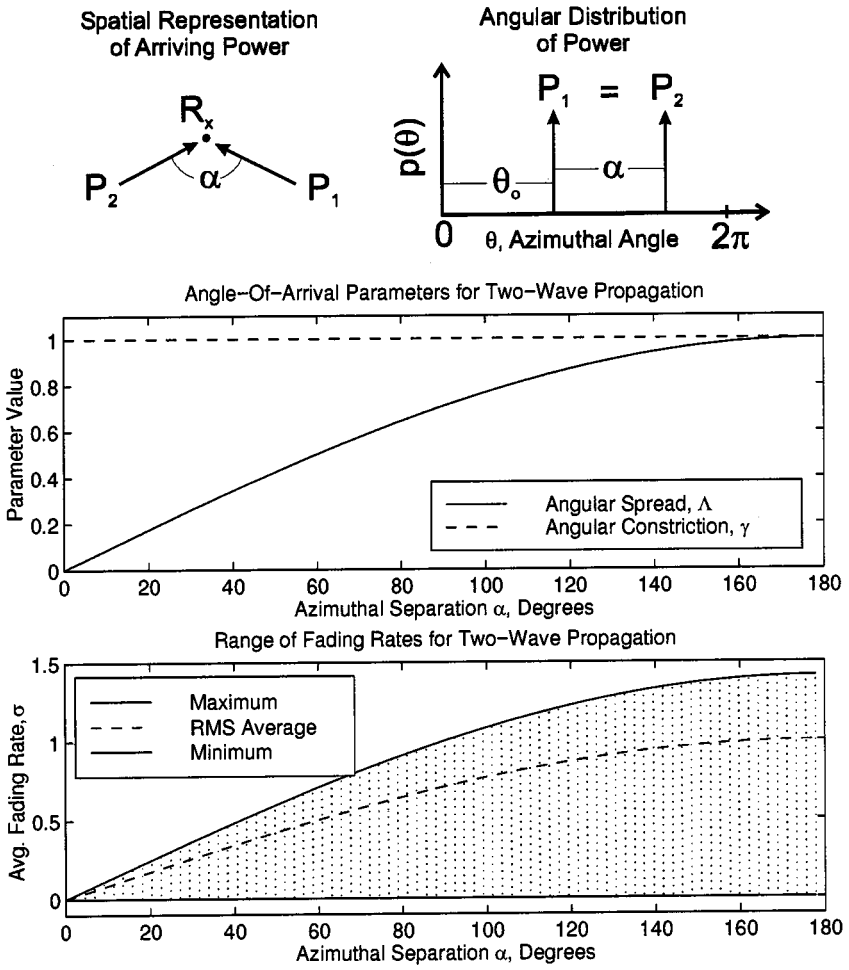


Fig. 1. Fading properties of two multipath components of equal power.

shows how the fading behavior changes as multipath separation angle $\alpha$ increases for the case of two equal-powered waves. Thus, increasing $\alpha$ changes a channel with low spatial selectivity into a channel with high spatial selectivity that exhibits a strong dependence on the azimuthal direction of receiver motion.

### *B. Sector Channel Model*

Consider another theoretical situation where multipath power is arriving continuously and uniformly over a range of azimuth angles. This model has been used to describe propagation for directional receiver antennas with a distinct azimuthal beam [7]. The function $p(\theta)$ will be defined by

$$p(\theta) = \begin{cases} \dfrac{P_T}{\alpha}, & \theta_o \le \theta \le \theta_o + \alpha \\ 0, & \text{elsewhere.} \end{cases} \tag{14}$$

The angle $\alpha$ indicates the width of the sector (in radians) of arriving multipath power and the angle $\theta_o$ is an arbitrary offset angle, as illustrated by Fig. 2. By applying (2)–(4), the expressions for $\Lambda$, $\gamma$, and $\theta_{\max}$ for this distribution are

$$\Lambda = \sqrt{1 - \frac{4\sin^2\frac{\alpha}{2}}{\alpha^2}}$$

$$\gamma = \frac{4\sin^2\frac{\alpha}{2} - \alpha\sin\alpha}{\alpha^2 - 4\sin^2\frac{\alpha}{2}}$$

$$\theta_{\max} = \theta_0 + \frac{\alpha+\pi}{2}. \tag{15}$$

The limiting cases of these parameters and (6) provide deeper understanding of angular spread and constriction.

Fig. 2 graphs the spatial channel parameter $\Lambda$ and $\gamma$ as a function of sector width $\alpha$. The limiting case of a single multipath arriving from precisely one direction corresponds to $\alpha = 0$, which results in the minimum angular spread of $\Lambda = 0$. The other limiting case of uniform illumination in all directions corresponds to $\alpha = 360°$ (omnidirectional Clarke model), which results in the maximum angular spread of $\Lambda = 1$. The angular constriction $\gamma$ follows an opposite trend. It is at a maximum ($\gamma = 1$) when $\alpha = 0$ and at a minimum ($\gamma = 0$) when $\alpha = 360°$. The graph in Fig. 2 shows that as the multipath angles of arrival are

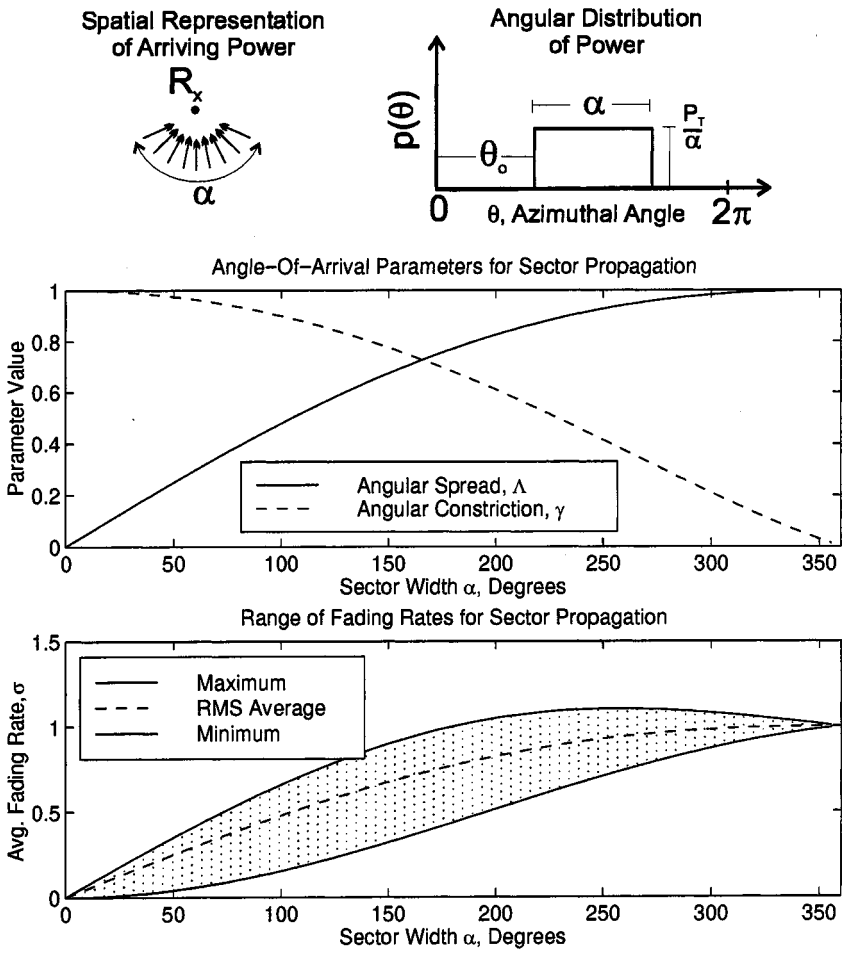


Fig. 2. Fading properties of a continuous sector of multipath components.

condensed into a smaller and smaller sector, the directional dependence of fading rates within the same local area increases. Overall, however, fading rates decrease with decreasing sector size $\alpha$.

### C. Double Sector Channel Model

Another example of angular constriction may be studied using the double sector model of Fig. 3. Diffuse multipath propagation over two equal and opposite sectors of azimuthal angles characterize the incoming power. The equation that describes this angular distribution of power is

$$p(\theta) = \begin{cases} \dfrac{P_T}{2\alpha}, & \theta_o \le \theta \le \theta_o + \alpha,\ \theta_o + \pi \le \theta \le \theta_o + \alpha + \pi \\ 0, & \text{elsewhere.} \end{cases} \tag{16}$$

The angle $\alpha$ is the sector width and the angle $\theta_o$ is an arbitrary offset angle. By applying (2)–(4), the expressions for $\Lambda$, $\gamma$, and $\theta_{\max}$ for this distribution are

$$\Lambda = 1, \qquad \gamma = \frac{\sin\alpha}{\alpha}, \qquad \theta_{\max} = \theta_0 + \frac{\alpha}{2}. \tag{17}$$

Note that the value of angular spread $\Lambda$ is always one. Regardless of the value of $\alpha$, an equal amount of power arrives from opposite directions, producing no clear bias in the direction of multipath arrival.

The limiting case of $\alpha = 180°$ (omnidirectional propagation) results in an angular constriction of $\gamma = 0$. As $\alpha$ decreases, the angular distribution of power becomes more and more constricted. In the limit of $\alpha = 0$, the value of angular constriction reaches its maximum $\gamma = 1$. This case corresponds to the above-mentioned instance of two-wave propagation. Fig. 3 shows how the fading behavior changes as sector width $\alpha$ increases, making the fading rate more and more isotropic while the RMS average remains constant.

### D. Rician Channel Model

A Rician channel model results from the addition of a single plane wave and numerous diffusely scattered waves [3]. If the power of the scattered waves is assumed to be evenly distributed in azimuth, then the channel may be modeled by the following $p(\theta)$:

$$p(\theta) = \frac{P_T}{2\pi(K+1)}\left[1 + 2\pi K\delta(\theta - \theta_0)\right] \tag{18}$$

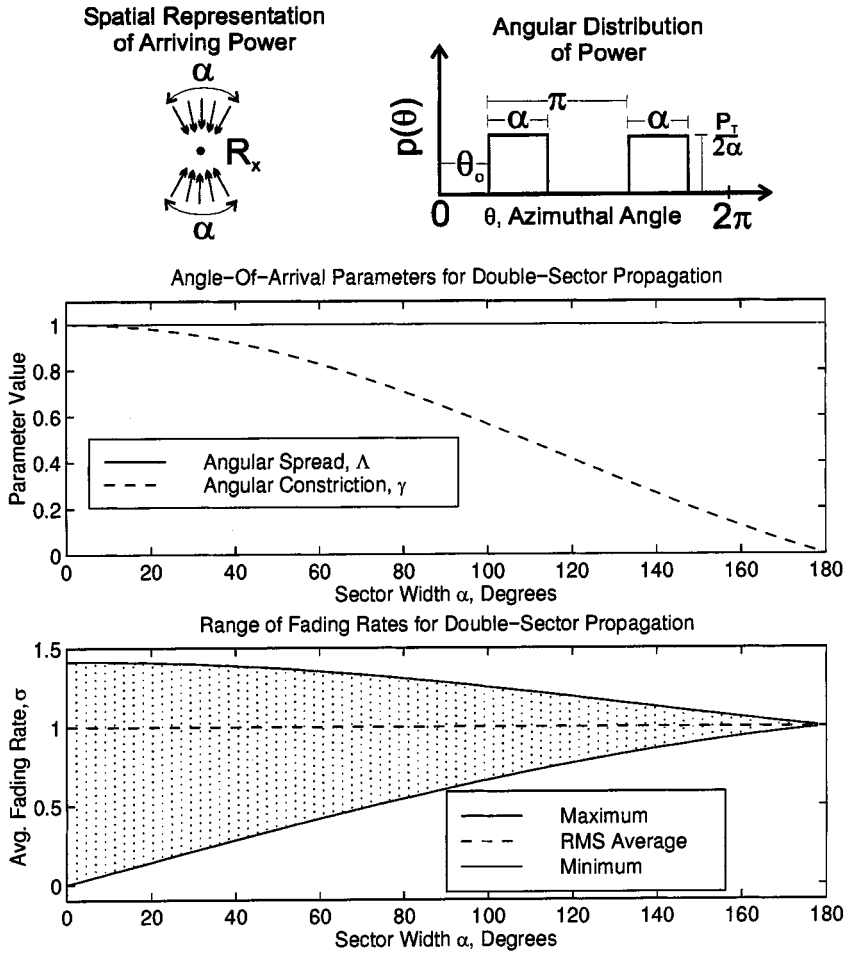


Fig. 3. Fading properties of double-sectored multipath components.

where $K$ is the ratio of coherent to diffuse incoherent power, often referred to as the Rician $K$-factor. By applying (2)–(4), the expressions for $\Lambda$, $\gamma$, and $\theta_{\max}$ for this distribution are

$$\Lambda = \frac{\sqrt{2K+1}}{K+1}, \qquad \gamma = \frac{K}{2K+1}, \qquad \theta_{\max} = \theta_0. \tag{19}$$

Fig. 4 depicts the spatial channel parameters $\Lambda$ and $\gamma$ as a function of $K$-factor. For very small $K$-factors, the channel appears to be omnidirectional ($\Lambda = 1$ and $\gamma = 0$). As the $K$-factor increases, the angular spread of the Rician channel decreases and the angular constriction increases. This indicates that the overall fading rate in the Rician channel decreases and that the differences between the minimum and maximum fading rate variances within the same local area but different directions increases.

## V. Second-Order Statistics Using Shape Factors

With an understanding of how shape factors describe fading rate variances, it is possible to redrive many of the basic second-order statistical measures of fading channels in terms of the three shape factors. Level-crossing rates, average fade duration, spatial autocovariance, and coherence distance expressions that were originally derived under the assumption of omnidirectional multipath propagation will now be cast in terms of the angular spread, the angular constriction, and the azimuthal direction of maximum fading [12], [19], [20].

The derivations focus on Rayleigh channels since these types of channels are analytically tractable. A Rayleigh fading signal is one whose envelope $R$ follows a Rayleigh PDF $f_R(r)$ given by

$$f_R(r) = r\sqrt{\frac{2}{P_T}}\exp\left(\frac{-r^2}{P_T}\right), \qquad r \geq 0 \tag{20}$$

where $P_T$ is the average total power received in a local area (units of *volts squared*).

### A. Level-Crossing Rates and Average Fade Duration

The general expression for a level-crossing rate is given by the following [2]:

$$N_R = \int_0^\infty \dot{r} f_{R\dot{R}}(R, \dot{r})\, d\dot{r} \tag{21}$$

where $R$ is the threshold level and $f_{R\dot{R}}(R, \dot{r})$ is the joint PDF of envelope and its time derivative. For a Rayleigh-fading signal, the level-crossing rate of the envelope process is

$$N_R = \frac{\rho\sigma_{\dot{V}}}{\sqrt{\pi P_T}}\exp(-\rho). \tag{22}$$

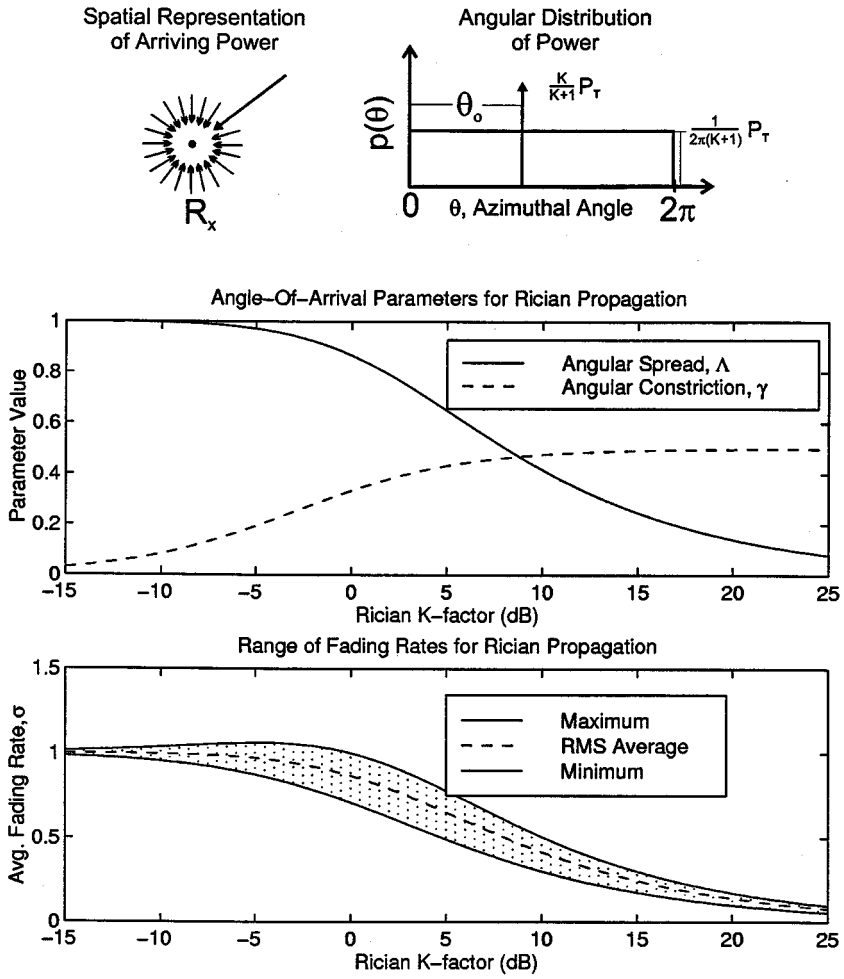


Fig. 4. Fading properties of Rician-model multipath components.

The variable $\rho$ is the normalized threshold level such that $\rho = R^2/P_T$ [2]. Note that $\sigma^2_{\dot{V}}$ is simply the time-derivative equivalent of $\sigma^2_{\dot{V}'}$ derived in Appendix I-A, which arises from a mobile receiver traveling through space with a constant velocity in an otherwise static channel (transmitter and scatterers are fixed).

By substituting (5) into (22), we arrive at an exact expression for the level-crossing rate in a Rayleigh fading channel with any arbitrary spatial distribution of multipath power and any direction of mobile receiver travel $\theta$

$$N_R = \frac{\sqrt{2\pi}v\Lambda\rho}{\lambda}\sqrt{1+\gamma\cos[2(\theta-\theta_{\max})]}\exp(-\rho^2). \quad (23)$$

The average fade duration $\overline{\tau}$ is defined to be [2], [6]

$$\overline{\tau} = \frac{1}{N_R}\int_0^R f_R(r)\,dr. \quad (24)$$

Substitution of the Rayleigh PDF of (20) and (23) into (24) yields

$$\overline{\tau} = \frac{\lambda[\exp(\rho^2)-1]}{\sqrt{2\pi}v\rho\Lambda\sqrt{1+\gamma\cos[2(\theta-\theta_{\max})]}}. \quad (25)$$

Equations (23) and (25) are useful tools for studying small-scale fading statistics in the presence of nonomnidirectional multipath.

### B. Spatial Autocovariance

Another important second-order statistic is the spatial autocovariance of received voltage envelope. The autocovariance function determines the correlation of received voltage envelope as a function of change in receiver position and is useful for studies in spatial diversity [2], [21]. Appendix II develops an approximate expression for the spatial autocovariance function of envelope based on shape factors [19]. The approximation reads

$$\rho(r,\theta) \approx \exp\left[-23\Lambda^2(1+\gamma\cos[2(\theta-\theta_{\max})])\left(\frac{r}{\lambda}\right)^2\right]. \quad (26)$$

Equation (26) allows us to estimate the envelope correlation between two points in space separated by a distance $r$ along an azimuthal direction $\theta$. The behavior of (26) is benchmarked in Section V-D against several known analytical solutions presented in [2].

### C. Coherence Distance

*Coherence distance* $D_c$ is the separation distance in space over which a fading channel appears to be unchanged. Coherence distance is important in the design of wireless receivers that employ spatial diversity to combat spatial selectivity. For mobile receivers, a similar parameter called *coherence time* $T_c$ is the elapsed time over which a fading channel appears to be constant. For the case of a static channel, the coherence time of a mobile receiver may be calculated from the coherence distance ($T_c = D_c/v$, where $v$ is the speed of the mobile).

Definitions for coherence distance may be based on the envelope autocovariance function. A convenient definition for the coherence distance $D_c$ is the value that satisfies the equation $\rho(D_c) = 0.5$ [22]. The classical value for coherence distance in an omnidirectional Rayleigh channel is given by

$$D_c \approx \frac{9\lambda}{16\pi} \tag{27}$$

where $\lambda$ is the wavelength of radiation. Using the generalized autocovariance function of (26) leads to a new definition of coherence distance

$$D_c \approx \frac{\lambda\sqrt{\ln 2}}{\Lambda\sqrt{23(1+\gamma\cos[2(\theta-\theta_{\max})])}}. \tag{28}$$

For omnidirectional propagation, (28) differs from (27) by only $-3.0\%$. Furthermore, (28) captures the behavior of nonomnidirectional propagation. As angular spread $\Lambda$ decreases, the coherence distance in a local area increases. As the angular constriction $\gamma$ increases, the coherence distance develops a strong dependence on orientation $\theta$.

### D. Revisiting Classical Channel Models

As a point of comparison, this section analyzes three well-known cases of propagation that have analytical solutions [2]. The cases are analyzed using the shape factor approach as outlined above for mobile receivers with speed $v$. This approach is shown to produce quick, comprehensive, and, most importantly, accurate solutions.

The first case corresponds to a narrowband receiver operating in a local area with multipath arriving from all directions such that the angular distribution of power $p(\theta)$ is a constant. The receiver antenna is assumed to be an omnidirectional whip, oriented perpendicular to the ground. Due to the vertical electric-field polarization of the whip antenna, this propagation scenario is referred to as the $E_z$ case [6].

The second two cases correspond to the same narrowband receiver in the same omnidirectional multipath channel, but with a small loop antenna mounted atop the receiver such that the plane of the loop is perpendicular to the ground. The antenna pattern of the small loop antenna attenuates the arriving multipath such that the angular distribution of power becomes

$$p(\theta) = A\sin^2\theta \tag{29}$$

where $A$ is some arbitrary gain constant. Unlike the omnidirectional $E_z$ case, the statistics of this propagation scenario will depend on the direction of travel by the receiver. The $H_x$ case will refer to a receiver traveling in a direction perpendicular to the main lobes of the loop antenna pattern ($\theta = 0$). The $H_y$ case will refer to a receiver traveling in a direction parallel to the main lobes ($\theta = \pi/2$). Fig. 5 illustrates the $E_z$, $H_x$, and $H_y$ cases for the modeled receiver antennas.

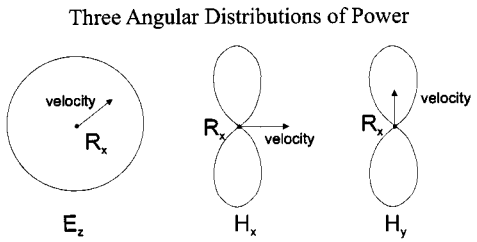


Fig. 5. Three different multipath-induced mobile-fading scenarios.

The first step is to calculate the three spatial parameters from the angular distribution of power $p(\theta)$ using (2)–(4). The spatial parameters for the $E_z$ case are $\Lambda = 1$, $\gamma = 0$, and $\theta_{\max} = 0$. Since this case is omnidirectional, the angular spread is at a maximum ($\Lambda = 1$) and the angular constriction is at a minimum ($\gamma = 0$). For the $H_x$ and $H_y$ cases, the spatial parameters are $\Lambda = 1$, $\gamma = 1/2$, and $\theta_{\max} = \pi/2$. Since the impinging multipath have no clear bias in *one* direction, the angular spread is at a maximum just like the $E_z$ case. However, there is clearly a bias in *two* directions, resulting in an increased angular constriction of $\gamma = 1/2$.

After substitution of these parameters into (23) along with the appropriate direction of mobile travel, the level-crossing rates for the three cases become

$$E_z\text{:}\quad N_R = \frac{\sqrt{2\pi}v\rho}{\lambda}\exp(-\rho^2) \tag{30}$$

$$H_x\text{:}\quad N_R = \frac{\sqrt{\pi}v\rho}{\lambda}\exp(-\rho^2) \tag{31}$$

$$H_y\text{:}\quad N_R = \frac{\sqrt{3\pi}v\rho}{\lambda}\exp(-\rho^2)\,. \tag{32}$$

The corresponding average fade durations are

$$E_z\text{:}\quad \overline{\tau} = \frac{\lambda}{\sqrt{2\pi}v\rho}\left[\exp(\rho^2) - 1\right] \tag{33}$$

$$H_x\text{:}\quad \overline{\tau} = \frac{\lambda}{\sqrt{\pi}v\rho}\left[\exp(\rho^2) - 1\right] \tag{34}$$

$$H_y\text{:}\quad \overline{\tau} - \frac{\lambda}{\sqrt{3\pi}v\rho}\left[\exp(\rho^2) - 1\right]. \tag{35}$$

These expressions exactly match the original solutions presented by Clarke in [6].

Now substitute the channel shape factors into the approximate spatial autocovariance functions in (26). The results for the three cases are

$$E_z\text{:}\quad \rho(r) = \exp\left[-23\left(\frac{r}{\lambda}\right)^2\right] \tag{36}$$

$$H_x\text{:}\quad \rho(r) = \exp\left[-11.5\left(\frac{r}{\lambda}\right)^2\right] \tag{37}$$

$$H_y\text{:}\quad \rho(r) = \exp\left[-34.5\left(\frac{r}{\lambda}\right)^2\right]. \tag{38}$$

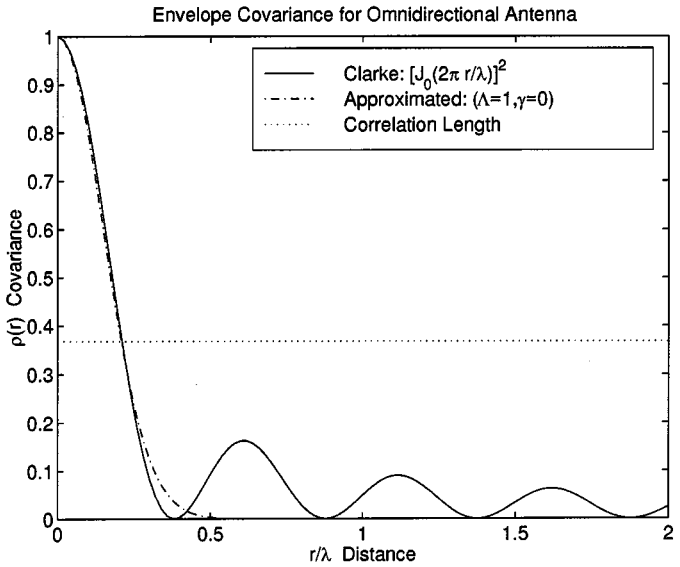


Fig. 6. Comparison between Clarke theoretical and approximate envelope autocovariance functions for $E_z$ case.

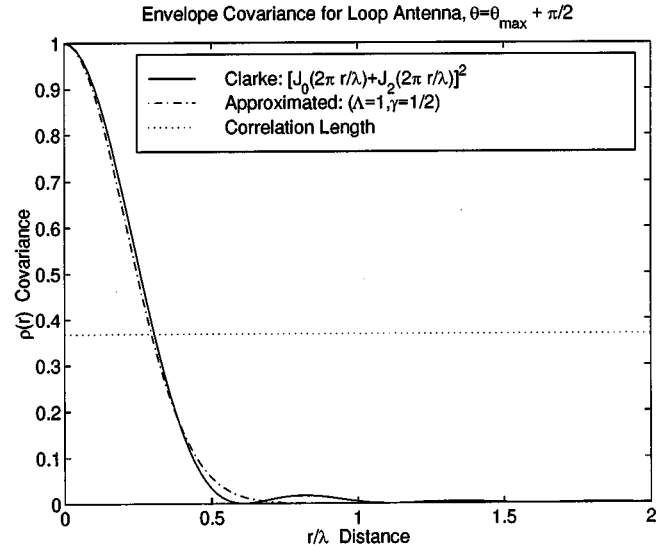


Fig. 7. Comparison between Clarke theoretical and approximate envelope autocovariance functions for $H_x$ case.

These three functions are compared to their more rigorous analytical solutions in Figs. 6–8. Note that all three model the spatial autocovariance function consistent with the approximation made in the derivation of (26). The behavior is nearly exact for values of $r$ equal to or less than a correlation distance.

### *E. Additional Comments*

The shape factor technique for finding fading statistics is an intuitive way to relate the physical channel characteristics to the fading behavior. In the previous examples, the spatial parameters may be calculated analytically or even estimated intuitively by simply looking at the distributions of multipath power in Fig. 5. The use of spatial parameters to find level crossing rate, average fade duration, and spatial autocovariance is quite simple when compared to the full analytical solutions of the $E_z$, $H_x$, and $H_y$ cases presented in [2]. The proposed solution is also more comprehensive. For example, once the shape factors have been found, (23), (25), and (26) provide statistics for *all* directions of travel for the $H_x$ and $H_y$ cases and not just specific directions such as $\theta = 0$ or $\theta = \pi/2$. Thus, specific fading behaviors for various directions of receiver motion are modeled easily.

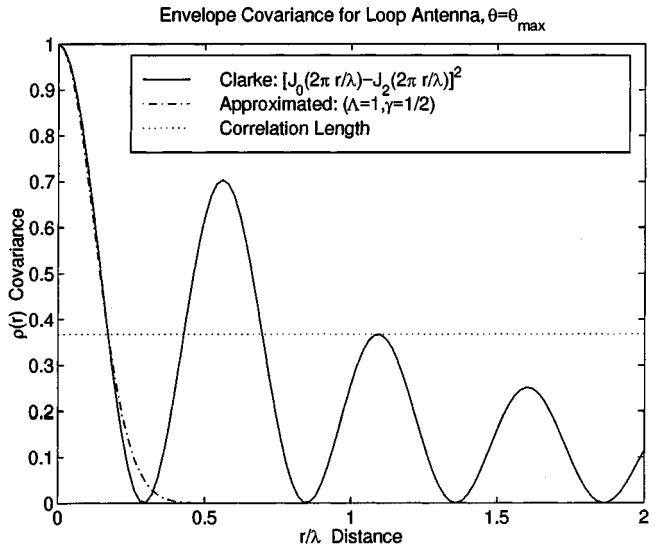


Fig. 8. Comparison between Clarke theoretical and approximate envelope autocovariance functions for $H_y$ case.

The solution form of (23), (25), and (26) reveals an interesting property about statistics in Rayleigh-fading channels. Since the three shape factors only depend on low-order Fourier coefficients, many of the second-order statistics of Rayleigh-fading channels are insensitive to the higher order multipath structure. The general biases of angular spread and angular constriction truly dominate the space and time evolution of these fading processes.

## VI. Conclusion

Multipath shape factor theory provides an easy, intuitive, and accurate method for analyzing small-scale fading channels with nonomnidirectional multipath propagation. The theory also has many implications for the measurement of wireless channels. For example, fading along specific directions may be measured in a local area with a simple noncoherent receiver to calculate various multipath angle-of-arrival characteristics. Conversely, angle-of-arrival characteristics may be measured with a directional antenna to calculate local area fading behavior.

The principle drawback of applying the theory to mobile receivers is the requirement of an otherwise static channel. If the fading induced by transient scatterers in the channel becomes large compared to the mobile-induced fading, then the theory may only be used to describe the spatial selectivity of a local area at a particular instant in time. Further work may also be required to extend the shape factor theory to situations where three-dimensional propagation becomes important rather than the classical two-dimensional (on-the-horizon) models that are typically used for terrestrial microwave propagation.

## APPENDIX I

This appendix derives the three rate variance relationships presented in this paper.

### A. Rate Variance for Complex Voltage

The power spectral density (PSD) of a base-band complex received voltage signal is related to the angular distribution of multipath power [7]

$$S_{\tilde{V}}(k) = \frac{2\pi\left[p\left(\theta + \cos^{-1}\frac{k}{k_{\max}}\right) + p\left(\theta - \cos^{-1}\frac{k}{k_{\max}}\right)\right]}{\sqrt{k_{\max}^2 - k^2}} \quad \text{for } |k| \le k_{\max} \tag{39}$$

where $\theta$ is the azimuthal direction of travel and $p(\cdot)$ is the angular distribution of impinging multipath power. The value $k_{\max}$ is the maximum wavenumber, which is equal to $2\pi/\lambda$. Note that the PSD is a function of wavenumber $k$ instead of frequency $\omega$ since multipath angles-of-arrival directly relate to *spatial* selectivity. By extension, the PSD is identical to the *doppler spectrum* $S_{\tilde{V}}(\omega)$ of a mobile receiver if the receiver moves in a static channel.

The second moment of the fading process is given by the following integration [2]:

$$\sigma_{\tilde{V}'}^2 = \frac{1}{2\pi}\int_{-k_{\max}}^{k_{\max}} (k - k_c)^2 S_{\tilde{V}}(k)\, dk \tag{40}$$

where $k_c$ is the centroid of the PSD

$$k_c = \frac{1}{2\pi F_0}\int_{-k_{\max}}^{k_{\max}} k S_{\tilde{V}}(k)\, dk. \tag{41}$$

$F_0$ is defined by (1)—this really just the average power of the process.

Now insert (41) into (40), making the change of variable $\theta_x = \theta \pm \cos^{-1}(k/k_{\max})$, where the $+$ and $-$ signs correspond to the left and right terms of $p(\cdot)$, respectively, of (39). After rearranging the limits of integration, the equation for $\sigma_{\tilde{V}'}^2$ becomes

$$\sigma_{\tilde{V}'}^2 = \frac{F_0 k_{\max}^2}{2} - \frac{k_{\max}^2}{F_0}\left[\int_0^{2\pi} p(\theta_x)\cos(\theta - \theta_x)\, d\theta_x\right]^2 + \frac{k_{\max}^2}{2}\left[\int_0^{2\pi} p(\theta_x)\cos[2(\theta - \theta_x)]\, d\theta_x\right]. \tag{42}$$

Consider a complex Fourier expansion of $\sigma_{\tilde{V}'}^2$ with respect to $\theta$

$$\sigma_{\tilde{V}'}^2 = \frac{1}{2\pi}\text{Real}\left\{\sum_{n=0}^{\infty} A_n \exp(jn\theta)\right\} = \frac{A_0}{2\pi} + \frac{1}{2\pi}\text{Real}\{A_2 \exp(j2\theta)\}. \tag{43}$$

All of the $A_n$ are zero for odd $n$. This is because $\sigma_{\tilde{V}'}(\theta) = \sigma_{\tilde{V}'}(\theta + \pi)$; that is, a 180° change in the direction of mobile travel should produce identical statistics. Furthermore, (42) has no harmonic content with respect to $\theta$ for $n > 2$. Solving for the only two remaining complex coefficients produces

$$A_0 = \int_0^{2\pi} \sigma_{\tilde{V}'}^2\, d\theta = \pi k_{\max}^2\left[F_0 - \frac{|F_1|^2}{F_0}\right] = \pi k_{\max}^2 \Lambda^2 E\left\{|\tilde{V}|^2\right\} \tag{44}$$

$$A_2 = 2\int_0^{2\pi} \sigma_{\tilde{V}'}^2 \exp(-j2\theta)\, d\theta = \pi k_{\max}^2\left[F_2 - \frac{F_1^2}{F_0}\right]^* = A_0 \gamma \exp(-j2\theta_{\max}) \tag{45}$$

where $\Lambda$, $\gamma$, and $\theta_{\max}$ are the three basic spatial channel parameters defined in (2)–(4). If these two coefficients are placed back into (43), the end result is the relationship for $\sigma_{\tilde{V}'}^2$ in (5).

For a mobile receiver, it is often convenient to measure the fading rate variance in terms of change per unit time instead of distance. If the mobile receiver operates in an otherwise static channel, then the mean-squared time rate-of-change $\sigma_{\dot{\tilde{V}}}^2$ is equal to $\sigma_{\tilde{V}'}^2$ multiplied by the squared velocity of the receiver.

### B. Rate Variance for Power

The stochastic process of power is defined as $P(r) = \tilde{V}^*(r)\tilde{V}(r)$. Thus, the PSD of power for $k \neq 0$ is the convolution of two complex voltage PSD's: $S_P(k) = (1/2\pi)S_{\tilde{V}}(k) \otimes S_{\tilde{V}}(-k)$, provided the complex voltage $\tilde{V}(r)$ is a Gaussian process (the condition for Rayleigh fading) [23]. The rate variance relationship for power may then be written as

$$\sigma_{P'}^2 = \frac{1}{2\pi}\int_{-\infty}^{\infty} k^2 S_P(k)\, dk \tag{46}$$

$$= \frac{1}{2\pi}\int_{-\infty}^{\infty} k^2\left[\frac{1}{2\pi}\int_{-\infty}^{\infty} S_{\tilde{V}}(\lambda)S_{\tilde{V}}(\lambda - k)\, d\lambda\right] dk. \tag{47}$$

Making the substitution $k = \lambda - k'$ leads to

$$\sigma_{P'}^2 = \frac{1}{4\pi^2}\int_{-\infty}^{\infty}\int_{-\infty}^{\infty} (\lambda - k')^2 S_{\tilde{V}}(\lambda)S_{\tilde{V}}(k')\, dk'\, d\lambda \tag{48}$$

which may be regrouped and re-expressed in terms of the spectral centroid $k_c$

$$\sigma_{P'}^2 = 2\underbrace{\left[\frac{1}{2\pi}\int_{-\infty}^{\infty} S_{\tilde{V}}(k)\, dk\right]}_{P_T}\underbrace{\left[\frac{1}{2\pi}\int_{-\infty}^{\infty} (k - k_c)^2 S_{\tilde{V}}(k)\, dk\right]}_{\sigma_{\tilde{V}'}^2}. \tag{49}$$

Now simply substitute (5) for $\sigma_{\tilde{V}'}^2$ to obtain (6).

### C. Rate Variance for Envelope

Based on the power relationship $P(r) = R^2(r)$, it is possible to write the following:

$$E\left\{\left(\frac{dP}{dr}\right)^2\right\} = 4E\{P(r)\}E\left\{\left(\frac{dR}{dr}\right)^2\right\} \tag{50}$$

which is valid for a Rayleigh fading process since $R$ and its derivative are independent [3]. Setting the left-hand side of (50) equal to the rate variance relationship for power in (6) produces the mean-squared fading rate result for a Rayleigh-fading voltage envelope in (7).

## APPENDIX II

### APPROXIMATE SPATIAL AUTOCOVARIANCE FUNCTION

This appendix derives the approximate spatial autocovariance function for small-scale Rayleigh fading signals.

The spatial autocovariance function for received envelope is defined as follows [2], [24]:

$$\rho(r) = \frac{E\{R(\vec{r}_o)R(\vec{r}_o + r\hat{r})\} - (E\{R\})^2}{E\{R^2\} - (E\{R\})^2} \tag{51}$$

where $\vec{r}_o$ is a position in the plane of the horizon (arbitrary if the fading process is considered to be wide-sense stationary) and $\hat{r}$ is a unit vector pointing in the direction of receiver travel $\theta$. To develop an approximate expression for the autocovariance of multipath fields, first expand the function $\rho(r)$ into a Mclaurin series

$$\rho(r) = \sum_{n=0}^{\infty} \frac{r^{2n}}{(2n)!} \left. \frac{d^{2n}\rho(r')}{dr'^{2n}} \right|_{r'=0}. \tag{52}$$

Equation (52) contains only even powers of $r$ since any real autocovariance function is an even function. The differentiation of an autocovariance function satisfies the following relationship [23]:

$$\left. \frac{d^{2n}}{dr^{2n}} E\{R(\vec{r}_o)R(\vec{r}_o + r\hat{r})\} \right|_{r=0} = (-1)^n E\left\{ \left( \frac{d^n R}{dr^n} \right)^2 \right\} \tag{53}$$

and is useful for re-expressing the Mclaurin series

$$\begin{aligned} \rho(r) &= 1 + \frac{\displaystyle\sum_{n=1}^{\infty} \frac{(-1)^n r^{2n}}{(2n)!} E\left\{ \left( \frac{d^n R}{dr^n} \right)^2 \right\}}{E\{R^2\} - (E\{R\})^2} \\ &= 1 - \frac{\displaystyle E\left\{ \left( \frac{dR}{dr} \right)^2 \right\}}{2[E\{R^2\} - (E\{R\})^2]} r^2 + \cdots \\ &= 1 - \frac{\displaystyle \frac{\pi^2}{\lambda^2} \Lambda^2 (1 - \gamma \cos[2(\theta - \theta_{\max})]) P_T}{\displaystyle 2\left(1 - \frac{\pi}{4}\right) P_T} r^2 + \cdots. \end{aligned} \tag{54}$$

Now consider $\rho(r)$ approximated by an arbitrary Gaussian function and its Mclaurin expansion

$$\begin{aligned} \rho(r) &\approx \exp\left[ -a\left( \frac{r}{\lambda} \right)^2 \right] \\ &\approx \sum_{n=0}^{\infty} \frac{(-1)^n a^n}{n!} \left( \frac{r}{\lambda} \right)^{2n} \\ &\approx 1 - a\left( \frac{r}{\lambda} \right)^2 + \cdots. \end{aligned} \tag{55}$$

A Gaussian function is chosen as a generic approximation to the true autocovariance since it is a convenient and well-behaved correlation function. The appropriate constant $a$ is chosen by setting equal the second terms of (54) and (55), ensuring that the behavior of both autocovariance functions is identical for small $r$

$$a = \underbrace{\left[ \frac{2\pi^2}{4 - \pi} \right]}_{\approx 23.00} \Lambda^2 (1 - \gamma \cos[2(\theta - \theta_{\max})]). \tag{56}$$

Therefore, the approximate spatial autocovariance depends only on the three multipath shape factors, as shown in (26).

## REFERENCES


[1] T. S. Rappaport, *Wireless Communications: Principles and Practice*. Englewood Cliffs, NJ: Prentice-Hall, 1996.

[2] W. C. Jakes, Ed., *Microwave Mobile Communications*. New York: IEEE Press, 1974.

[3] S. O. Rice, "Statistical properties of a sine wave plus random noise," *Bell Syst. Tech. J.*, vol. 27, no. 1, pp. 109–157, Jan. 1948.

[4] H. Suzuki, "A statistical model for urban radio propagation," *IEEE Trans. Commun.*, vol. 25, pp. 673–680, July 1977.

[5] A. J. Coulson, A. G. Williamson, and R. G. Vaughan, "A statistical basis for log-normal shadowing effects in multipath fading channels," *IEEE Trans. Commun.*, vol. 46, pp. 494–502, Apr. 1998.

[6] R. H. Clarke, "A statistical theory of mobile-radio reception," *Bell Syst. Tech. J.*, vol. 47, pp. 957–1000, 1968.

[7] M. J. Gans, "A power-spectral theory of propagation in the mobile radio environment," *IEEE Trans. Veh. Technol.*, vol. VT-21, pp. 27–38, Feb. 1972.

[8] J.-P. Rossi, J.-P. Barbot, and A. J. Levy, "Theory and measurement of the angle of arrival and time delay of UHF radiowaves using a ring array," *IEEE Trans. Antennas Propagat.*, vol. 45, pp. 876–884, May 1997.

[9] J. Fuhl, J.-P. Rossi, and E. Bonek, "High-resolution 3-D direction-of-arrival determination for urban mobile radio," *IEEE Trans. Antennas Propagat.*, vol. 45, pp. 672–682, Apr. 1997.

[10] J. H. Winters, "Smart antennas for wireless systems," *IEEE Personal Commun.*, vol. 1, pp. 23–27, Feb. 1998.

[11] J. C. Liberti and T. S. Rappaport, *Smart Antennas for Wireless CDMA Communications*. Englewood Cliffs, NJ: Prentice-Hall, 1999.

[12] G. D. Durgin and T. S. Rappaport, "Three parameters for relating small-scale temporal fading to multipath angles-of-arrival," in *PIMRC'99*, Osaka, Japan, Sept. 1999, pp. 1077–1081.

[13] ——, "A basic relationship between multipath angular spread and narrow-band fading in a wireless channel," *Inst. Elect. Eng. Electron. Lett.*, vol. 34, pp. 2431–2432, Dec. 1998.

[14] Y. Ebine, T. Takahashi, and Y. Yamada, "A study of vertical space diversity for a land mobile radio," *Electron. Commun. Jpn.*, vol. 74, no. 10, pp. 68–76, 1991.

[15] A. F. Naguib and A. Paulraj, "Performance of wireless CDMA with $M$-ary orthogonal modulation and cell site arrays," *IEEE J. Selected Areas Commun.*, vol. 14, pp. 1770–1783, Dec. 1996.

[16] T. Fulghum and K. Molnar, "The Jakes fading model incorporating angular spread for a disk of scatterers," in *48th IEEE Veh. Technol. Conf.*, Ottawa, Canada, May 1998, pp. 489–493.

[17] S.-S. Jeng, G. Xu, H.-P. Lin, and W. J. Vogel, "Experimental studies of spatial signature variation at 900 MHz for smart antenna systems," *IEEE Trans. Antennas Propagat.*, vol. 46, pp. 953–962, July 1998.

[18] N. Patwari, G. D. Durgin, T. S. Rappaport, and R. J. Boyle, "Peer-to-peer low antenna outdoor radio wave propagation at 1.8 GHz," in *49th IEEE Veh. Technol. Conf.*, vol. 1, Houston, TX, May 1999, pp. 371–375.

[19] G. D. Durgin and T. S. Rappaport, "Effects of multipath angular spread on the spatial cross-correlation of received voltage envelopes," in *49th IEEE Veh. Technol. Conf.*, vol. 2, Houston, TX, May 1999, pp. 996–1000.

[20] ——, "Level crossing rates and average fade duration of wireless channels with spatially complicated multipath," in *Globecom'99*, Brazil, Dec. 1999.

[21] R. G. Vaughan and N. L. Scott, "Closely spaced monopoles for mobile communications," *Radio Sci.*, vol. 28, no. 6, pp. 1259–1266, Nov. Dec. 1993.

[22] R. Steele, *Mobile Radio Communications.* Piscataway, NJ: IEEE Press, 1994.
[23] A. Papoulis, *Probability, Random Variables, and Stochastic Processes*, 3rd ed. New York: McGraw-Hill, 1991.
[24] A. M. D. Turkmani, A. A. Arowojolu, P. A. Jefford, and C. J. Kellett, "An experimental evaluation of the performance of two-branch space and polarization diversity schemes at 1800 MHz," *IEEE Trans. Veh. Technol.*, vol. 44, pp. 318–326, May 1995.

**Gregory D. Durgin** (S'99) was born in Baltimore, MD, on October 23, 1974. He received the B.S.E.E. and M.S.E.E. degrees from Virginia Polytechnic Institute and State University, Blacksburg, VA, in 1996 and 1998, respectively. He is currently working toward the Ph.D. degree at the Mobile and Posrable Radio Research Group (MPRG) at the same university as a Bradley Fellow.

Since 1996, he has been a Research Assistant at MPRG, where his research focuses on radio wave propagation, channel measurement, and applied electromagnetics. He has published (as a student) 14 technical papers in international journals and conferences. He serves regularly as a consultant to industry.

Mr. Durgin received the 1998 Blackwell Award for best graduate research presentation in the Electrical and Computer Engineering Department, Virginia Polytechnic Institute and State University. He also received the 1999 Stephen O. Rice Prize as a coauthor with T. S. Rappaport and H. Xu for the best original research paper published in the IEEE TRANSACTIONS ON COMMUNICATIONS.

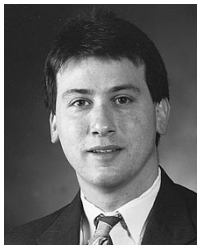

**Theodore S. Rappaport** (S'83 –M'87 –SM'91–F'98) received the B.S.E.E., M.S.E.E., and Ph.D. degrees from Purdue University, West Lafayette, IN, in 1982, 1984, and 1987, respectively.

Since 1988, he has been on the Virginia Polytechnic Institute and State University electrical and computer engineering faculty, where he is the James S. Tucker Professor and Founding Director of the Mobile and Portable Radio Research Group (MPRG), a university research and teaching center dedicated to the wireless communications field. In 1989 he founded TSR Technologies, Inc., a cellular radio/PCS manufacturing firm, which he sold in 1993. He is Chairman of Wireless Valley Communications, Inc., has consulted for over 20 multinational corporations, and has served the International Telecommunications Union as a consultant for emerging nations. He holds three patents and has authored, coauthored, and coedited 14 books in the wireless field, including *Wireless Communications: Principles and Practice* (Englewood Cliffs, NJ: Prentice-Hall, 1996), *Smart Antennas for Wireless Communications: IS-95 and Third Generation CDMA Applications* (Englewood Cliffs, NJ: Prentice-Hall, 1999), and several compendia of papers including "Cellular Radio and Personal Communications: Selected Readings" (IEEE Press, 1995, "Cellular Radio and Personal Communications: Advanced Selected Readings" (IEEE Press, 1996), and "Smart Antennas: Selected Readings (IEEE Press, 1998). He has coauthored more than 130 technical journal and conference papers. He serves on the editorial board of *International Journal of Wireless Information Networks*.

Dr. Rappaport received the Marconi Young Scientist Award in 1990 and an NSF Presidential Faculty Fellowship in 1992. He was the recipient of the 1998 IEEE Communications Society Stephen O. Rice Prize Paper Award. He is active in the IEEE Communications and Vehicular Technology societies. He is a registered professional engineer in Virginia and is a past member of the Board of Directors of the Radio Club of America.